

**CASE FILE
COPY**

N 62 13947

NASA TN D-1370

**TECHNICAL NOTE**

D-1370

NUMERICAL ANALYSIS OF THE
TRANSIENT RESPONSE OF ADVANCED THERMAL PROTECTION SYSTEMS
FOR ATMOSPHERIC ENTRY

By Robert T. Swann and Claud M. Pittman

Langley Research Center
Langley Station, Hampton, Va.

FACILITY FORM 602

N62-13947
(ACCESSION NUMBER)
40
(PAGES)
TN-DI-370
(NASA CR OR TMX OR AD NUMBER)

1
(THRU)
02
(CODE)
02
(CATEGORY)

NATIONAL AERONAUTICS AND SPACE ADMINISTRATION
WASHINGTON

July 1962



NATIONAL AERONAUTICS AND SPACE ADMINISTRATION

TECHNICAL NOTE D-1370

NUMERICAL ANALYSIS OF THE
TRANSIENT RESPONSE OF ADVANCED THERMAL PROTECTION SYSTEMS
FOR ATMOSPHERIC ENTRY

By Robert T. Swann and Claud M. Pittman

SUMMARY

Equations for the transfer of heat through thermal protection shields are derived in finite difference form. These equations are applicable to charring ablators, impregnated ceramics, subliming ablators, heat sinks, and insulating materials and have been programmed for solution on a high-speed digital computer. In the program, thermal properties can be functions of temperature. Provision is made for analysis of heat shields subjected to simultaneous convective and radiative heat inputs. Some typical results are presented. Limited comparisons with experimental results are made.

INTRODUCTION

An adequate thermal protection system may constitute 20 to 30 percent of the total reentry weight for vehicles which must enter the earth's atmosphere at supercircular velocity. Preliminary studies (ref. 1) indicate that charring ablators and impregnated ceramics will provide the most efficient thermal protection shield for a major portion of the vehicle. Therefore, a more detailed analysis of the performance of such shields is desirable.

Extensive experimental investigations have been conducted on the performance of charring ablators (refs. 2, 3, and 4). However, most of this work has been concerned with overall performance of the material in the given environment. Consequently, little information of a fundamental nature is available concerning char layers. For example, several mechanisms can be postulated for the removal of char at the surface, such as oxidation, vaporization, and shear or thermal stress. However, precise analytical expressions for the rate of char removal by such mechanisms are not available. Therefore, an analytical program must have considerable flexibility if it is to be suitable for investigation of the various mechanisms that may be operative.

In this paper, equations are derived for calculating the thermal response of charring ablators and impregnated ceramics to reentry heating conditions. The equations have been programmed for an IBM 7090 electronic data processing system, and numerical examples are presented.

SYMBOLS

C_{i+j}, C_{i+j+m}	heat capacity of heat sink	L
c_p	specific heat	1
\bar{c}_p	specific heat of gaseous products of pyrolysis	3
F	heat generation function	5
g	initial temperature distribution	9
H_c	heat of ablation of outer material	
H_p	blocking effectiveness of gaseous products of pyrolysis	
h_e	local enthalpy external to boundary layer	
h_w	local enthalpy of fluid at wall	
Δh_c	heat capacity of coolant	
Δh_p	heat of pyrolysis	
i	number of stations in char, including one at each surface	
j	number of stations in uncharred material, including one at back face	
k	thermal conductivity	
l	distance between stations	
M	molecular weight of gaseous products of pyrolysis	
m	number of stations in insulation, including one at back surface	
\dot{m}	mass-loss rate	

\dot{m}_c	rate of char loss
\dot{m}_p	rate of loss of uncharred material
q	actual heating rate at surface
q_c	convective heating rate to a cold wall with no mass transfer
q_R	radiant heating rate
$s(\theta - \bar{T})$	unit step function: $S = 0, \theta < \bar{T}; S = 1, \theta \geq \bar{T}$
T	temperature
T_B	temperature to which back surface radiates
T_n	temperatures of the finite difference stations
\bar{T}_i	temperature of pyrolysis
$\bar{T}_{i+j}, \bar{T}_{i+j+m}$	temperature at which cooling system is activated
\bar{T}_1	temperature at which char ablates
t	time
w_c	total weight of coolant used
Δw_c	rate of coolant consumption
x	thickness
x	distance from initial outer surface to outer surface of char layer
y	distance from initial outer surface of char layer
Δy	increment in the space variable
z	distance from back surface of shield
α_c	weighting factor for transpiration effectiveness of char mass loss

α_p	weighting factor for transpiration effectiveness of pyrolysis products, $\left(\frac{M_{air}}{M}\right)^{1/4}$	
ϵ	emissivity	
θ	differential temperature	
ρ	density	
σ	Stefan-Boltzmann constant	L 1 3 5 9
Subscripts:		
o	initial value	
i, j, m, n	integers	

Unprimed symbols refer to char layer, unless otherwise specified; single primes refer to uncharred material; and double primes refer to insulation.

ANALYSIS

The thermal protection system that is to be analyzed is shown schematically in figure 1. Although this discussion is confined to a charring ablator system, all the concepts and equations apply equally as well to any other thermal protection system composed of not more than three primary layers. For a charring ablator system the outer (heated) layer is the char, the center layer contains the uncharred material, and the third layer consists of insulation.

The outer surface may or may not erode depending on the material and the aerodynamic conditions. Pyrolysis of the uncharred material may occur at the interface between the char and the uncharred material. Theoretically, it is anticipated that pyrolysis will occur over some range of temperatures and positions, but in this analysis it is assumed that pyrolysis occurs at a single location and at a temperature which is a known function of time or of rate of pyrolysis. Thus a well-defined interface is assumed to exist between the charred and uncharred material. Erosion of the char surface and pyrolysis at the char-uncharred material interface results in two moving boundaries. The presence of these moving boundaries distinguishes the current problem from standard heat-transfer analyses.

The material that is liberated by erosion of the outer surface and pyrolysis at the interface, enters the boundary layer and causes a

significant reduction in aerodynamic heating. It has been shown (refs. 5, 6, and 7) that, for moderate mass-transfer rates, the effectiveness of mass transfer in blocking aerodynamic heating is approximately a linear function of the enthalpy in the flow outside the boundary layer. It is further shown in references 7 and 8, however, that this approximation may lead to serious error if the surface is exposed to a net radiant heat input, such as that which a typical vehicle would experience from reentry at parabolic or hyperbolic velocities.

Blocking effectiveness as a function of a mass-transfer-rate parameter $\frac{\dot{m}_{he}}{q_C}$ is shown in figure 2. It can be seen from figure 2 that the usual linear approximation for a laminar boundary layer is not valid at higher values of mass-transfer-rate parameter. The effect of radiant heating is to increase \dot{m} , which results in operation at higher values of $\frac{\dot{m}_{he}}{q_C}$. The exact solution was obtained from the boundary-layer solutions for air-to-air injection (ref. 8). The second-degree approximation was developed by fitting a curve at values of $\frac{\dot{m}_{he}}{q_C}$ of 0, 1.0, and 2.5. The equation for the second-degree approximation is

$$\frac{q}{q_C} = 1 - 0.724h_e \left(\frac{\alpha_c \dot{m}_c + \alpha_p \dot{m}_p}{q_C} \right) + 0.13h_e^2 \left(\frac{\alpha_c \dot{m}_c + \alpha_p \dot{m}_p}{q_C} \right)^2; \quad \left. \begin{cases} \left(h_e \left(\frac{\alpha_c \dot{m}_c + \alpha_p \dot{m}_p}{q_C} \right) < 2.5 \right) \\ \left(h_e \left(\frac{\alpha_c \dot{m}_c + \alpha_p \dot{m}_p}{q_C} \right) \geq 2.5 \right) \end{cases} \right\} \quad (1)$$

$$\frac{q}{q_C} = 0; \quad \left. \begin{cases} \left(h_e \left(\frac{\alpha_c \dot{m}_c + \alpha_p \dot{m}_p}{q_C} \right) < 2.5 \right) \\ \left(h_e \left(\frac{\alpha_c \dot{m}_c + \alpha_p \dot{m}_p}{q_C} \right) \geq 2.5 \right) \end{cases} \right\}$$

The equations have been formulated to provide the option of using either a heat of ablation such as the linear function of enthalpy (ablation theory) or a second-degree approximation to the actual blocking effectiveness (transpiration theory).

Very little experimental data is available at high mass-transfer rates, and in conservative calculations it may be desirable to specify a minimum value of q/q_C greater than 0. This approach would certainly be in order if boundary-layer separation is found to occur at high mass-injection rates. The constants α_c and α_p are used to correct equations (1) for the difference between the molecular weight of the boundary-layer gas and the molecular weight of the injected gas. The constant α_c must also be corrected for that part of the char that is removed from the

surface mechanically, that is, for the char that is removed but not vaporized. A similar approach might be used to correct for turbulent flow. The effects of molecular weight and turbulent flow are discussed in reference 9.

The mechanism of char erosion has not been established at this time, and it may be desirable to use any of the following mechanisms:

- (1) Ablation at a given temperature
- (2) Erosion rate as a given function of time (resulting, for example, from oxidation of the char)
- (3) Erosion occurring at such a rate that the char thickness is a given function of time (resulting, for example, from mechanical erosion of the char)

L
1
3
5
9

Evidence indicates that oxidation is the primary means of char removal in the ground facility tests conducted at the Langley Research Center.

To simplify the analysis, the following assumptions are introduced:

- (1) Pyrolysis occurs at a single given temperature, so that a well-defined interface exists between the char layer and the uncharred material.
- (2) Thermal properties are functions of temperature only.
- (3) All heat flow is normal to the surface.
- (4) Gases transpiring through the char are at the same temperature as the char.

In general, the char surface and the char-uncharred material interface are moving with respect to the back surface. Therefore, it is necessary to formulate expressions for the locations of the boundaries between the different layers with reference to a fixed coordinate system. It is convenient to select a stationary coordinate system with the origin located at the initial char surface. Then the distances between the initial outer surface and the various boundaries between layers can be determined from figure 1. The distance between the outer surface of the char and the initial outer surface is

$$\bar{x} = \int_0^{t_f} \frac{\dot{m}_c}{\rho} dt \quad (2a)$$

The distance between the char-uncharred material interface and the initial outer surface is

$$\bar{x} + x = x_0 + \int_0^t \frac{\dot{m}_p}{\rho' - \rho} dt \quad (2b)$$

The distance between the initial outer surface and the back surface of the uncharred material is

$$x_0 + x'_0 = \text{Constant} \quad (2c)$$

L
1
3
5
9

The distance between the initial outer surface and the back surface of the system is

$$x_0 + x'_0 + x''_0 = \text{Constant} \quad (2d)$$

The instantaneous thicknesses of the three layers are, respectively,

$$\left. \begin{aligned} x &= x_0 + \int_0^t \frac{\dot{m}_p}{\rho' - \rho} dt - \int_0^t \frac{\dot{m}_c}{\rho} dt \\ x' &= x'_0 - \int_0^t \frac{\dot{m}_p}{\rho' - \rho} dt \\ x'' &= x''_0 \end{aligned} \right\} \quad (3)$$

The actual charring ablator shield used on the reentry vehicle will, of course, not develop a char layer until the surface reaches the pyrolysis temperature. However for purposes of the analysis it is necessary to start the calculations with a finite char thickness. If a very thin char layer is used, this procedure will have a negligible influence on the final result.

Differential Equations and Boundary Conditions

Differential equations governing the transfer of heat within the three layers can be derived now without further approximation. They are:

$$\frac{\partial}{\partial y} \left(k \frac{\partial \theta}{\partial y} \right) + \dot{m}_p \bar{c}_p \frac{\partial \theta}{\partial y} + F = \rho c_p \frac{\partial \theta}{\partial t}$$

Heat conducted Heat absorbed by the Heat generated Heat stored
transpiring gases

$$(\bar{x} \leq y \leq \bar{x} + x) \quad (4a)$$

$$\frac{\partial}{\partial y} \left(k' \frac{\partial \theta'}{\partial y} \right) = \rho' c'_p \frac{\partial \theta'}{\partial t} \quad (\bar{x} + x \leq y \leq x_o + x'_o) \quad (4b)$$

$$\frac{\partial}{\partial y} \left(k'' \frac{\partial \theta''}{\partial y} \right) = \rho'' c''_p \frac{\partial \theta''}{\partial t} \quad (x_o + x'_o \leq y \leq x_o + x'_o + x''_o) \quad (4c)$$

The initial condition is

$$\theta(y, 0) = g(y) \quad (5)$$

Considerable generality is necessary in the boundary conditions if the equations are to have the required versatility. The heat transfer to the outer surface is assumed to be a given function of time, consisting of the cold-wall convective heating rate q_C and the radiant heating rate q_R incident on the surface. These two components must be specified separately, because mass transfer at the surface blocks part of the aerodynamic heating but in general has no effect on radiant heating.

The boundary condition at $y = \bar{x}$ is

$$q_C \left(1 - \frac{h_w}{h_e} \right) \left\{ 1 - (1 - \beta) \left[0.724 \frac{h_e}{q_C} \left(\alpha_c \dot{m}_c + \alpha_p \dot{m}_p \right) - 0.13 \left(\frac{h_e}{q_C} \right)^2 \left(\alpha_c \dot{m}_c + \alpha_p \dot{m}_p \right)^2 \right] \right\} + q_R = \sigma \epsilon_1 \theta^4 - k \frac{\partial \theta}{\partial y} + \beta S(\theta - \bar{T}_1) \dot{m}_c H_c + \beta \dot{m}_p H_p \quad (6)$$

where $\beta = 0$ or 1 depending on whether transpiration or ablation theory is used to evaluate the blocking effect. Equation (6) is normally used in this analysis as the boundary condition on the temperature at the outer surface. However, when θ is equal to the ablation temperature \bar{T}_1 the specified ablation temperature provides the boundary condition

on the temperature and equation (6) is used to calculate the rate of ablation \dot{m}_c . The coefficients α_c and α_p can be used to differentiate between the blocking effectiveness of material evolved at the outer surface and at the char-uncharred material interface. Note the limitation imposed on the transpiration term by equation (1).

At the char-uncharred material interface, $y = \bar{x} + x$

$$\theta = \theta'$$

and

$$-k \frac{\partial \theta}{\partial y} = S(\theta' - \bar{T}_i) \dot{m}_p \Delta h_p - k' \frac{\partial \theta'}{\partial y} \quad (7)$$

The rate of pyrolysis \dot{m}_p is calculated from equation (7) subject to the restriction

$$\dot{m}_p = 0 \quad (8a)$$

if

$$\theta_{y=\bar{x}+x} < \bar{T}_i \quad (8b)$$

When pyrolysis is occurring, the boundary conditions on the temperatures at the interface are:

$$\theta = \theta' = \bar{T}_i \quad (8c)$$

Provision is made to impose several conditions at the back surface of the shield. This surface can be perfectly insulated or subjected to any combination of heat sink, cooling, or radiative transfer. These conditions apply to either a two- or three-layer system depending on whether or not insulation is used. Furthermore, it is possible to insert a heat-sink condition at the back of the second layer whether or not a third layer is used. When cooling is used, the temperature at which the cooling system is activated must be given and the amount of coolant necessary to keep the surface at a specified temperature is calculated.

If the third layer is not used, the back-surface boundary condition is

$$-k' \frac{\partial \theta'}{\partial y} = C_{i+j} \frac{\partial \theta'}{\partial t} + S(\theta' - \bar{T}_{i+j}) \Delta W_C \Delta h_C + \sigma \epsilon_{i+j} \left[(\theta')^4 - T_B^4 \right] \quad (9)$$

The choice of conditions is accomplished by making the unwanted terms 0 (i.e., $C_{i+j} = 0$ and/or $\bar{T}_{i+j} > \bar{T}_1$ and/or $\epsilon_{i+j} = 0$).

If the third layer is used, the boundary condition at the interface between the second and third layers is

$$\theta' = \theta''$$

$$-k' \frac{\partial \theta'}{\partial y} = C_{i+j} \frac{\partial \theta'}{\partial t} - k'' \frac{\partial \theta''}{\partial y} \quad (10)$$

At the back surface,

$$y = x_O + x_O' + x_O''$$

and the boundary condition is

$$-k'' \frac{\partial \theta''}{\partial y} = C_{i+j+m} \frac{\partial \theta''}{\partial t} + S(\theta'' - \bar{T}_{i+j+m}) \Delta W_C \Delta h_C + \sigma \epsilon_{i+j+m} \left[(\theta'')^4 - T_B^4 \right] \quad (11)$$

Finite Difference Equations

The system of equations (eqs. (1) to (11)) is extremely complicated (nonlinear with variable coefficients) and solutions in analytic form are hardly to be expected. The systems can be put into a form suitable for numerical calculation by deriving the equations in finite difference form from heat-balance considerations.

It is convenient to space the finite difference stations at equal intervals throughout a given layer, as shown in figure 3. Let the first layer contain i stations, including one at the front and one at the back surface of the first material. The second layer contains j stations including one at the back surface of the second material. The

third layer contains m stations including one at the back surface. Then the distances between stations are

$$\left. \begin{aligned} l &= \frac{x}{i-1} \\ l' &= \frac{x'}{j} \\ l'' &= \frac{x''}{m} \end{aligned} \right\} \quad (12)$$

L
1
3
5
9

for the three layers.

The heat-transfer equations are as follows:

$$\begin{aligned} q_C \left(1 - \frac{h_w}{h_e} \right) \left\{ 1 - (1 - \beta) \left[0.724 \frac{h_e}{q_C} \left(\alpha_C \dot{m}_C + \alpha_p \dot{m}_p \right) - 0.13 \left(\frac{h_e}{q_C} \right)^2 \left(\alpha_C \dot{m}_C + \alpha_p \dot{m}_p \right)^2 \right] \right\} \\ + q_R = k_{1,2} \frac{T_1 - T_2}{l} + \sigma \epsilon_1 T_1^4 + \beta S (T_1 - \bar{T}_1) \dot{m}_C H_C + \dot{m}_p \left(\bar{c}_{p,1} \frac{T_1 - T_2}{2} + \beta H_p \right) \\ - F_1 + \frac{\rho_1 c_{p,1} l}{2} \frac{dT_1}{dt} \end{aligned} \quad (13)$$

$$k_{n-1,n} \frac{T_{n-1} - T_n}{l} - k_{n,n+1} \frac{T_n - T_{n+1}}{l} - \dot{m}_p \bar{c}_{p,n} \frac{T_{n-1} - T_{n+1}}{2} + F_n = \rho_n c_{p,n} l \frac{dT_n}{dt} \quad (n = 2, 3, \dots, i-1) \quad (14)$$

$$\begin{aligned} k_{i-1,i} \frac{T_{i-1} - T_i}{l} - k'_{i,i+1} \frac{T_i - T_{i+1}}{l'} - \dot{m}_p S (T_i - \bar{T}_i) \left(\bar{c}_{p,i} \frac{T_{i-1} - T_i}{2} + \Delta h_p \right) \\ + F_i = \left(\frac{\rho_i c_{p,i} l}{2} + \frac{\rho'_i c'_{p,i} l'}{2} \right) \frac{dT_i}{dt} \end{aligned} \quad (15)$$

$$k'_{n-1,n} \frac{T_{n-1} - T_n}{l'} - k'_{n,n+1} \frac{T_n - T_{n+1}}{l'} = \rho'_n c'_{p,n} l' \frac{dT_n}{dt}$$

$$(n = i + 1, i + 2, \dots, i + j - 1) \quad (16)$$

For two layers,

$$k'_{i+j-1,i+j} \frac{T_{i+j-1} - T_{i+j}}{l'} = \left(\rho'_{i+j} c'_{p,i+j} \frac{l'}{2} + c_{i+j} \right) \frac{dT_{i+j}}{dt}$$

$$+ S \left(T_{i+j} - \bar{T}_{i+j} \right) \Delta W_C \Delta h_C + \sigma \epsilon_{i+j} \left(T_{i+j}^4 - T_B^4 \right) \quad (17)$$

For three layers,

$$k'_{i+j-1,i+j} \frac{T_{i+j-1} - T_{i+j}}{l'} - k''_{i+j,i+j+1} \frac{T_{i+j} - T_{i+j+1}}{l''}$$

$$= \left(\rho'_{i+j} c'_{p,i+j} \frac{l'}{2} + \rho''_{i+j} c''_{p,i+j} \frac{l''}{2} + c_{i+j} \right) \frac{dT_{i+j}}{dt} \quad (18)$$

$$k''_{n-1,n} \frac{T_{n-1} - T_n}{l''} - k''_{n,n+1} \frac{T_n - T_{n+1}}{l''} = \rho''_n c''_{p,n} l'' \frac{dT_n}{dt}$$

$$(n = i + j + 1, i + j + 2, \dots, i + j + m - 1) \quad (19)$$

$$k''_{i+j+m-1,i+j+m} \frac{T_{i+j+m-1} - T_{i+j+m}}{l''}$$

$$= \left(\rho''_{i+j+m} c''_{p,i+j+m} \frac{l''}{2} + c_{i+j+m} \right) \frac{dT_{i+j+m}}{dt}$$

$$+ S \left(T_{i+j+m} - \bar{T}_{i+j+m} \right) \Delta W_C \Delta h_C + \sigma \epsilon_{i+j+m} \left(T_{i+j+m}^4 - T_B^4 \right) \quad (20)$$

The temperature rise rate of the station n is

$$\frac{dT_n}{dt} = \frac{\partial T_n}{\partial t} + \frac{\partial T_n}{\partial y} \frac{\partial y}{\partial t} \quad (21a)$$

or

$$\Delta T_n = \left(\frac{\partial T_n}{\partial t} + \frac{\partial T_n}{\partial y} \frac{\partial y}{\partial t} \right) \Delta t \quad (21b)$$

Then the temperatures at $t + \Delta t$ are

$$T_1(t + \Delta t) = T_1 + \frac{dT_1}{dt} \Delta t \quad (22a)$$

$$T_n(t + \Delta t) = T_n + \frac{dT_n}{dt} \Delta t + \frac{T_{n+1} - T_{n-1}}{2x} \left[(i - n) \frac{\dot{m}_c}{\rho} + (n - 1) \frac{\dot{m}_p}{\rho' - \rho} \right] \Delta t \quad (n = 2, 3, \dots, i - 1) \quad (22b)$$

$$T_i(t + \Delta t) = T_i + \frac{dT_i}{dt} \Delta t \quad (22c)$$

$$T_n(t + \Delta t) = T_n + \frac{dT_n}{dt} \Delta t + \frac{T_{n+1} - T_{n-1}}{2x'} \left[(1 + j - n) \frac{\dot{m}_p}{\rho' - \rho} \right] \Delta t \quad (n = i + 1, i + 2, \dots, i + j - 1) \quad (22d)$$

$$T_n(t + \Delta t) = T_n + \frac{dT_n}{dt} \Delta t \quad (n = i + j, i + j + 1, \dots, i + j + m) \quad (22e)$$

All of the temperatures on the right-hand side of equation (22) are evaluated at the time t . The time derivatives are calculated explicitly from the finite difference equations (eqs. (13) to (20)).

Calculation of Temperatures at Fixed Points

It is possible to calculate the temperature at any number of fixed points Z_n where Z is the distance from the back surface. The temperature at Z_n is calculated as follows (using linear interpolation):

When

$$0 < Z_n \leq x''$$

find station N such that

$$(i + j + m - N)\ell'' \geq Z_n \geq (i + j + m - N - 1)\ell''$$

Then

$$T(Z_n) = T_N + (T_N - T_{N+1}) \frac{Z_n - (i + j + m - N)\ell''}{\ell''} \quad (23)$$

When

$$x'' \leq Z_n \leq x' + x''$$

find N such that

$$x'' + (i + j - N)\ell' \geq Z_n \geq x'' + (i + j - N - 1)\ell'$$

Then

$$T(Z_n) = T_N + (T_N - T_{N+1}) \frac{Z_n - x'' - (i + j - N)\ell'}{\ell'} \quad (24)$$

When

$$x' + x'' \leq z_n \leq x + x' + x''$$

find N such that

$$x' + x'' + (i - N)l \geq z_n \geq x' + x'' + (i - N - 1)l$$

L
1
3
5
9

Then

$$T(z_n) = T_N + (T_N - T_{N+1}) \frac{z_n - x' - x'' - (i - N)l}{l} \quad (25)$$

If the outside surface moves past the largest z_n being computed because of ablation of the surface, then the temperature at this point is meaningless and is, therefore, excluded in subsequent calculations.

Programming Procedures

Equations (13) to (20) and the required auxiliary relations have been programmed for a 32K two-channel IBM 7090 electronic data processing system. The program was constructed in FAP source language and designed to operate under control of the Fortran Monitor.

The primary difficulty encountered in using the program is the time required to obtain solutions on the digital computer. The equations are integrated stepwise over time, and the maximum time interval for which the solution is stable with the explicit formulation used is (ref. 10)

$$\Delta t = \frac{1}{2} \frac{(\Delta y)^2 \rho c_p}{k}$$

The initial value of Δy in the char is extremely small. In the physical case the initial value of Δy may be zero. However, in the calculations a finite initial char thickness is required. An initial char thickness of 0.001 foot has been selected as the smallest value for which computations are practical. The computing interval used with four elements in this thickness is

$$\Delta t = 2^{-10} \approx 0.001 \text{ sec}$$

When the char thickness increases as a result of the heating condition, the computing interval can be increased.

The inputs necessary to perform a calculation with the present routine are now described. Those inputs which can be tabulated as functions of time $f(t)$ or functions of temperature $f(T)$ are indicated. Any or all inputs may, of course, be made constant. When an input is not presently a function of time or temperature but might conveniently be made such a function it will be indicated. Note that the presence of thermal radiation makes it necessary to use an absolute temperature scale.

L
1
3
5
9

Trajectory inputs:

- (1) $h_e = h_e(t)$
- (2) $q_C = q_C(t)$
- (3) $q_R = q_R(t)$
- (4) Start and stop times

Material inputs:

- (1) $c_p, c'_p, c''_p, \bar{c}_p = f(T)$
- (2) $\rho, \rho', \rho'' = f(T)$
- (3) $k, k', k'' = f(T)$
- (4) $\epsilon_l, \epsilon_{i+j}, \epsilon_{i+j+m} = \text{Constant}$ (could be made $f(T)$)
- (5) $C_{i+j}, C_{i+j+m} = \text{Constant}$ (could be made $f(T)$)
- (6) $\Delta h_C = \text{Constant}$ (could be made $f(T)$)

Configuration inputs:

- (1) $x, x', x''; x'' = \text{Constant}$ (See miscellaneous input 1 for $x = f(t)$; an initial $x > 0$ must be used even if no char is actually present.)
- (2) $i, j, m = \text{Constant}$
- (3) $Z_n = \text{Constant}$

Miscellaneous inputs:

- (1) \bar{T}_1 , \dot{m} , or $x = f(t)$
- (2) \bar{T}_{i+j} , \bar{T}_{i+j+m} , $T_B = f(t)$
- (3) H_c , $H_p = f(t)$
- (4) $i + j + m$ initial temperatures
- (5) \dot{m}_c must be specified if $T_{1,o} = \bar{T}_1$ and \dot{m}_p must be specified if $T_{1,o} = \bar{T}_i$
- (6) α_c , α_p , and β

DISCUSSION OF ANALYSIS

The equations derived herein provide a means for determining the response of a thermal protection system to a reentry heating environment. The accuracy of the results obtained depends on the precision with which the reentry environment and thermal properties of the shield are specified.

The equations were derived primarily to provide a means for investigating the performance of charring ablators. However, the same equations are suitable for the analysis of impregnated ceramic, insulating ceramic, subliming, and heat-sink materials.

The equations are applicable only to one-dimensional heat flow, and problems which are essentially two or three dimensional (such as pyrolytic graphite in certain applications) cannot be treated. If a liquid layer is produced at the surface, the effect of this layer must be reduced to a heat of ablation form before calculations of the response of the system can be made.

A solution of the equations gives the response of a particular configuration to the given heat pulse. However, in design calculations, it is desired to obtain the minimum weight configuration for the given heat pulse, subject to the necessary factors of safety. Therefore several separate calculations are normally required for each reentry heating condition.

The extensive computer time required for each solution severely limits the number of solutions that can be obtained. A number of methods for reducing the required computer time have been considered. An alternate method of solution, the implicit formulation, in which the equations

are solved simultaneously, would permit the use of much larger time intervals since in this form the solution is unconditionally stable. However, the time required to obtain each solution would increase, and there would be some doubt as to the degree of accuracy of the results.

Another approach for reducing computer time is to neglect the heat storage terms of the equations having small Δy , which reduces computer time by an order of magnitude. A preliminary investigation indicates that this procedure will yield pyrolysis rates that are too high by 1 to 10 percent. This approach is particularly promising for optimum weight design studies, that is, the specific heat term can be neglected in preliminary calculations; then, when the optimum weight design is established, a more refined calculation can be made.

L
1
3
5
9

TYPICAL RESULTS

The analysis developed in the previous sections can be used to calculate the important parameters used in evaluating the thermal performance of a charring ablator during entry into a planetary atmosphere. Instantaneous temperature distributions and pyrolysis rates can be determined. From the state of the system at the end of the heating period, the required thermal protection weight can be estimated.

Before any calculations can be performed, the environmental heating conditions and the thermal properties of the heat shield must be specified. In this paper, a typical ballistic trajectory for reentry at parabolic velocity was selected. The trajectory and the corresponding heating rates are shown in figure 4. Both the radiative and convective components of the heating rate are shown, since they are used in the analysis as separate inputs.

The thermal protection system selected for this analysis is shown in figure 5. It consisted of a layer of phenolic-nylon (50 percent phenolic) bonded to a 1/2-inch-thick stainless-steel honeycomb-core sandwich panel structure with a cooling system beneath the structure. The phenolic-nylon material properties were selected from available data and from an analysis of the performance of this material in an arc-jet facility. The sandwich panel material properties were determined from available data with the effective thermal conductivity of the panel calculated from reference 11. The material properties used are presented in table I. The cooling system was assumed to maintain the adjacent honeycomb panel surface at 100° F with a consequent weight requirement calculated from equation (20). For the purposes of these calculations, the char layer was divided into 4 elements, the uncharred material was divided into 10 elements, and the insulation was divided into 4 elements.

There is considerable question as to the behavior of the char layer (which forms from the virgin phenolic-nylon material) when it is subjected to the flight environment. It is possible that the char may erode thermally, chemically, or mechanically or by any combination of these processes. Because of this the char-layer thickness was the primary variable in the input data. Four char-layer conditions were considered. In the first three cases the char layer was allowed to attain thicknesses of 0.05, 0.1, and 0.25 inch with no char removal, and then held constant at these values throughout the rest of the calculation. In the fourth case no char removal occurred.

The criterion which determined the initial thickness of ablator necessary for reentry with the given trajectory was that the bond line between the phenolic-nylon and the honeycomb panel not exceed a temperature of 600° F. *A priori* it could not be expected that an assumed initial thickness would exactly satisfy this requirement. However, for a given char-thickness condition and initial phenolic-nylon thickness, both temperature distributions and coolant required can be calculated and therefore the weight of the system can be determined. Then by making several calculations for the same char-thickness condition but with different initial phenolic-nylon thicknesses, a plot of bond-line temperature against weight can be made and the weight for a 600° F bond-line temperature determined. The four calculations discussed in this report had maximum bond-line temperatures between 500° and 600° F.

The preceding discussion indicates two important results which may be obtained from these calculations, that is, temperature distributions and thermal protection system weight. Another important result implicit in the determination of the other two is the mass-loss rate of the charring ablator. This mass loss occurs at the material interface and also, in three of the four cases, at the outer surface. Figures depicting these three parameters obtained from representative calculations of the four cases considered are discussed in the following sections.

Temperature Distributions

Temperature profiles through the charring ablator at selected times during reentry are shown in figure 6, for each of the maximum char thicknesses considered. The surface temperature as a function of surface position is indicated by the dashed line. These curves are plotted in a coordinate system having its origin at the original char surface. In figure 6(a), there is no char removal and the surface remains at its initial location. In figure 6(b) the maximum char thickness is 0.25 inch. No char is lost until the char thickness reaches this value. For example, it is clear that no char has been lost at 40 seconds because the temperature profile extends to the original outer-surface location. At 100 seconds,

the temperature distribution extends from a distance 0.15 inch from the original surface to the back surface. Therefore, 0.15 inch of char has been removed from the surface at the time 100 seconds after reentry heating began. Similarly, after 200 seconds, 0.47 inch of char has been removed. Figures 6(c) and 6(d) are similar to figure 6(b), except that the maximum char thicknesses are 0.10 and 0.05 inch, respectively. As expected, it can be seen that, at a given time, the amount of char removed increases as the maximum char thickness decreases.

As a result of the boundary condition at the interface between the char layer and the uncharred material (eq. (15)), there will, in general, be a discontinuity in the slope of the temperature profile at the interface. Such discontinuities do, in fact, exist in figure 6; although they are not noticeable because of the steepness of the curves.

Pyrolysis was assumed to occur at $1,250^{\circ}$ F. Therefore, the location of the interface between the char layer and the uncharred material can be determined if the temperature profile is available and if pyrolysis is still occurring. For example, from figure 6(b) pyrolysis has penetrated a distance 0.4 inch after 100 seconds of heating. If the temperature profile intersects the pyrolysis temperature at more than one point (fig. 6(a)), the pyrolysis interface must be at or beyond that intersection farthest from the outer surface.

L
1
3
5
9

Temperature Histories

Typical temperature histories are plotted in figure 7. The curves shown are for points located 0.5, 0.6, 0.7, and 0.8 inch from the original outer surface for the case in which the maximum char thickness is 0.25 inch. Each curve ends when the outer surface reaches the location of the given point. For example, a point 0.5 inch from the original outer surface becomes the pyrolyzing interface at 124 seconds ($1,250^{\circ}$ F) and progresses to the outer surface at 212 seconds. Similarly the points 0.6, 0.7, and 0.8 inch from the original outer surface become the outer surface at 500, 736, and 800 seconds, respectively. Note that the temperature at a specified location may decrease with time although the point in question is still approaching the receding outer surface. This is possible because of the sharp decrease in the heating rate (fig. 4(b)) during this time period.

A conclusion having considerable experimental significance can be drawn from these temperature history curves. An examination of the shape of the curves (fig. 7) in the vicinity of the pyrolysis interface temperature ($1,250^{\circ}$ F) reveals no discontinuities in the slope, thus there is no indication of the passage of the interface. Since this observation is made from curves computed with a specific pyrolysis temperature, it is extremely improbable that the location of the interface can be determined

from experimental temperature data since evidence indicates that pyrolysis actually occurs in an appreciable thickness over a range of temperature. Thus, some other method must be found if the location of the pyrolysis region is to be determined.

Rate of Pyrolysis

The rate of pyrolysis is plotted in figure 8 for each of the maximum char-thickness conditions considered. The lower curve gives the mass-loss rate for the case in which no char removal occurs. The mass-loss rates for the other char removal conditions are identical to that for no char removal, until the char thickness reaches its maximum value. With char thicknesses of 0.05 and 0.10 inch, the rate of pyrolysis is significantly higher than for 0.25 inch of char. The difference between the rate of pyrolysis with a maximum char thickness of 0.25 inch and with no char removal is relatively smaller. However, even in this case the rates of pyrolysis differ by a factor greater than two after the char thickness for the nochar-removal case has become appreciably greater than 0.25 inch.

Thermal-Protection-System Weight

The thermal-protection-system weight required to limit the temperature of the bond line to 600° F is shown in figure 9 as a function of char thickness. The weight of coolant required to maintain a 100° F interior temperature is included in the thermal-protection-system weight; however, the honeycomb panel is assumed to be a structural member and its weight is not included.

The required weight decreases rapidly with increasing maximum char thickness at the smaller values of maximum char thickness. At maximum char thicknesses of more than about 0.2 inch, the change in weight with maximum char thickness is much less significant. The required weight when no char is lost is indicated.

Measured values of char conductivity are not available. The values used in this analysis were estimated using transient test results, and may be in considerable error. The effect of doubling the thermal conductivity is shown by the top curve in figure 9.

Effect of Thermal Radiation

As shown in references 7 and 8 the effect of a net radiant heat input to a surface is to decrease the effectiveness of mass transfer in blocking the convective heat input. To determine the effect of radiation

on the weight requirement for the current trajectory, calculations were performed by using only the convective component of the heating with a maximum char thickness of 0.10 inch. The required weight was about 10 lb/sq ft as shown by the circle in figure 9. Therefore, the ratio of the weight required without incident radiation to the weight required with incident radiation is approximately equal to the ratio of the heat input without incident radiation to the heat input with incident radiation. The increase in the required weight is proportional to the increase in total heat input, and the effect of the radiant heat input is similar to the effect of an equivalent increase in the convective heat input. This result might be anticipated because of the high surface temperature; even with relatively high radiant heat inputs, the system operates with a net radiant heat output.

A limiting case in which the entire heat input is radiative (equal to the sum of the actual convective and radiative heating rates) has also been investigated. In this case, injection of the pyrolysis products into the boundary layer does not reduce the heat input to the surface. Consequently, the heating rate experienced by the surface during pyrolysis is much greater. The required weight for the all-radiative case is approximately 29 lb/sq ft; this is about 2.5 times as great as the weight required for the actual trajectory.

The effects of radiant heating on the performance of charring ablatives can be summarized as follows: When the radiant heating is a minor fraction of the total heating the required thermal protection system is approximately the same as if the total heat input were convective. When radiant heating is dominant, the effectiveness of this system is greatly reduced.

Comparison With Experiment

Considerable research has been done on the evaluation of thermal protection materials in an electric arc-powered air jet. When the thermal properties and ablation characteristics of the test material have been reasonably well-known, good agreement has been obtained between calculated and experimental results. Some success has been attained in determining uncertain material characteristics by attempting to match calculated and experimental results.

For the most part, effort has been concentrated on determining the variation of char conductivity with temperature that would result in the measured char thickness and that would match experimentally determined internal temperatures. Figure 10 shows a comparison of calculated and experimental temperature histories obtained with phenolic-nylon subjected to a cold-wall heating rate of about 100 Btu/ft²-sec. Temperature is plotted as a function of time for several stations measured from the back

L
1
3
5
9

surface. The solid curves are experimental temperature traces and the dashed curves are calculated results. The dashed curves shown in figure 10 are the best fit to the experimental results that has been obtained. It was found that the conductivity providing the best fit was a cubic function of temperatures. This variation of char conductivity with temperature was subsequently used in the calculations. (See table I.)

CONCLUDING REMARKS

The computer program, described in this report, is capable of providing a numerical analysis of charring ablator, impregnated ceramic, subliming, or heat-sink thermal protection systems, subjected to a severe heating environment. The accuracy of the results obtained is determined by the accuracy with which the environmental data, the materials properties data, and the ablation characteristics of the material in the environment are known. The principal limitation of the program is that considerable machine time is necessary to produce the average calculation. For materials whose thermal properties and ablation characteristics are fairly well-known, good agreement has been obtained between calculated and experimental results.

Langley Research Center,
National Aeronautics and Space Administration,
Langley Station, Hampton, Va., May 4, 1962.

REFERENCES

1. Swann, Robert T.: Composite Thermal Protection Systems for Manned Re-Entry Vehicles. ARS Jour., vol. 32, no. 2, Feb. 1962, pp. 221-226.
2. Brooks, William A., Jr.: Wadlin, Kenneth L., Swann, Robert T., and Peters, Roger W.: An Evaluation of Thermal Protection for Apollo. NASA TM X-613, 1961.
3. Schwartz, H. S. [compiler]: Conference on Behavior of Plastics in Advanced Flight Vehicle Environments. WADD Tech. Rep. 60-101, U.S. Air Force, Sept. 1960.
4. Schmidt, Donald L.: Behavior of Plastic Materials in Hyperthermal Environments. WADC Tech. Rep. 59-574, U.S. Air Force, Apr. 1960.
5. Roberts, Leonard: Mass Transfer Cooling Near the Stagnation Point. NASA TR R-8, 1959. (Supersedes NACA TN 4391.)
6. Roberts, Leonard: A Theoretical Study of Stagnation-Point Ablation. NASA TR R-9, 1959. (Supersedes NACA TN 4392.)
7. Swann, Robert T., and South, Jerry: A Theoretical Analysis of Effects of Ablation on Heat Transfer to an Arbitrary Axisymmetric Body. NASA TN D-741, 1961.
8. Swann, Robert T.: Effect of Thermal Radiation From a Hot Gas Layer on Heat of Ablation. Jour. Aerospace Sci. (Readers' Forum), vol. 28, no. 7, July 1961, pp. 582-583.
9. Savin, Raymond C., Gloria, Hermilo R., and Dahms, Richard G.: Ablative Properties of Thermoplastics Under Conditions Simulating Atmosphere Entry of Ballistic Missiles. NASA TM X-397, 1960.
10. Dusinberre, G. M.: Numerical Methods for Transient Heat Flow. Trans. A.S.M.E., vol. 67, no. 8, Nov. 1945, pp. 703-712.
11. Swann, Robert T., and Pittman, Claud M.: Analysis of Effective Thermal Conductivities of Honeycomb-Core and Corrugated-Core Sandwich Panels. NASA TN D-714, 1961.

TABLE I.- MATERIAL PROPERTIES

PHENOLIC-NYLON:

Char:

Density, lb/cu ft	17
Specific heat, Btu/lb-°R	0.5
Thermal conductivity, k, Btu/ft-sec-°R	$6.6 \times 10^{-6} \left(\frac{T}{1000} \right)^3$
Emissivity	0.8

L
1
3
5
9

Uncharred Material:

Density, lb/cu ft	75
Specific heat, Btu/lb-°R	0.38
Thermal conductivity, Btu/ft-sec-°R	4×10^{-5}

STAINLESS-STEEL HONEYCOMB-CORE SANDWICH PANEL:

Density, lb/cu ft	7.3
Specific heat, Btu/lb-°R	0.14
Thermal conductivity, k, Btu/ft-sec-°R, for -	

T = 400° R	4.3×10^{-5}
T = 500° R	4.33×10^{-5}
T = 600° R	4.41×10^{-5}
T = 700° R	4.55×10^{-5}
T = 800° R	4.65×10^{-5}
T = 900° R	4.74×10^{-5}
T = 1,000° R	4.82×10^{-5}
T = 1,100° R	4.89×10^{-5}
T = 1,200° R	5.02×10^{-5}
T = 1,300° R	5.10×10^{-5}
T = 1,400° R	5.18×10^{-5}
T = 2,000° R	6.01×10^{-5}

MISCELLANEOUS:

Specific heat of gaseous products of pyrolysis,
 \bar{c}_p , Btu/lb-°R, for -

T = 500° R	0.6
T = 2,000° R	0.6
T = 2,250° R	0.5
T = 2,500° R	0.4
T = 2,750° R	0.3
T = 6,000° R	0.3
Heat of pyrolysis, Btu/lb	650
Temperature of pyrolysis	1,710° R (1,250° F)

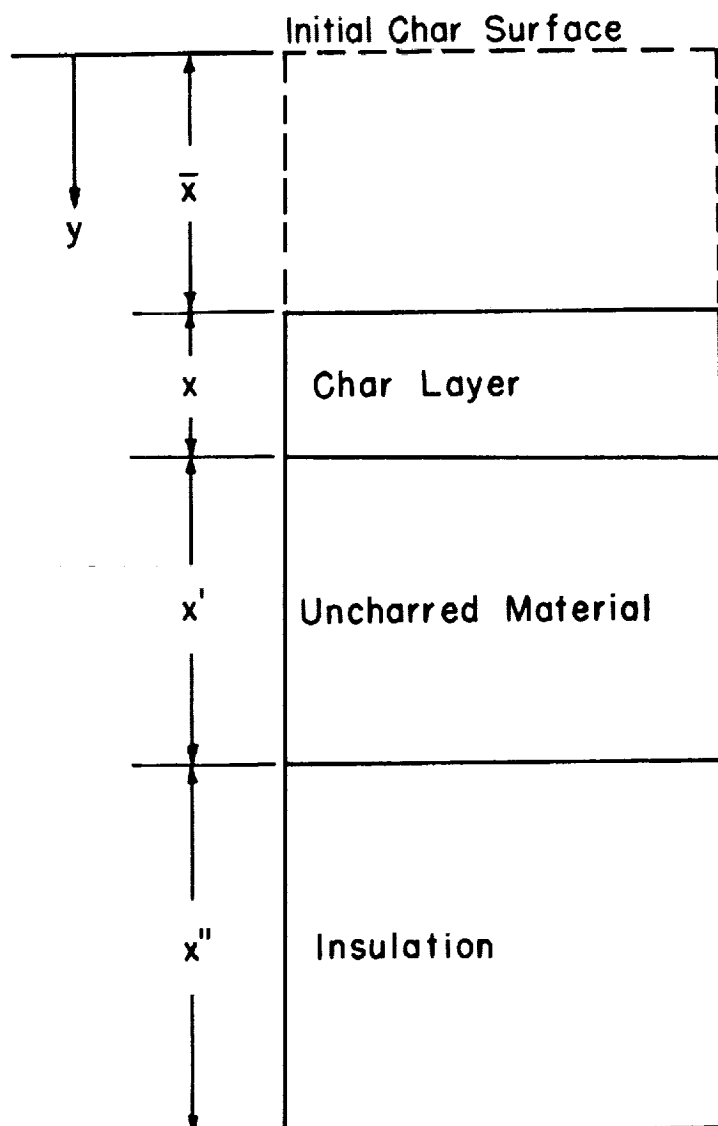


Figure 1.- Schematic diagram of system employing charring ablator.

L-1359

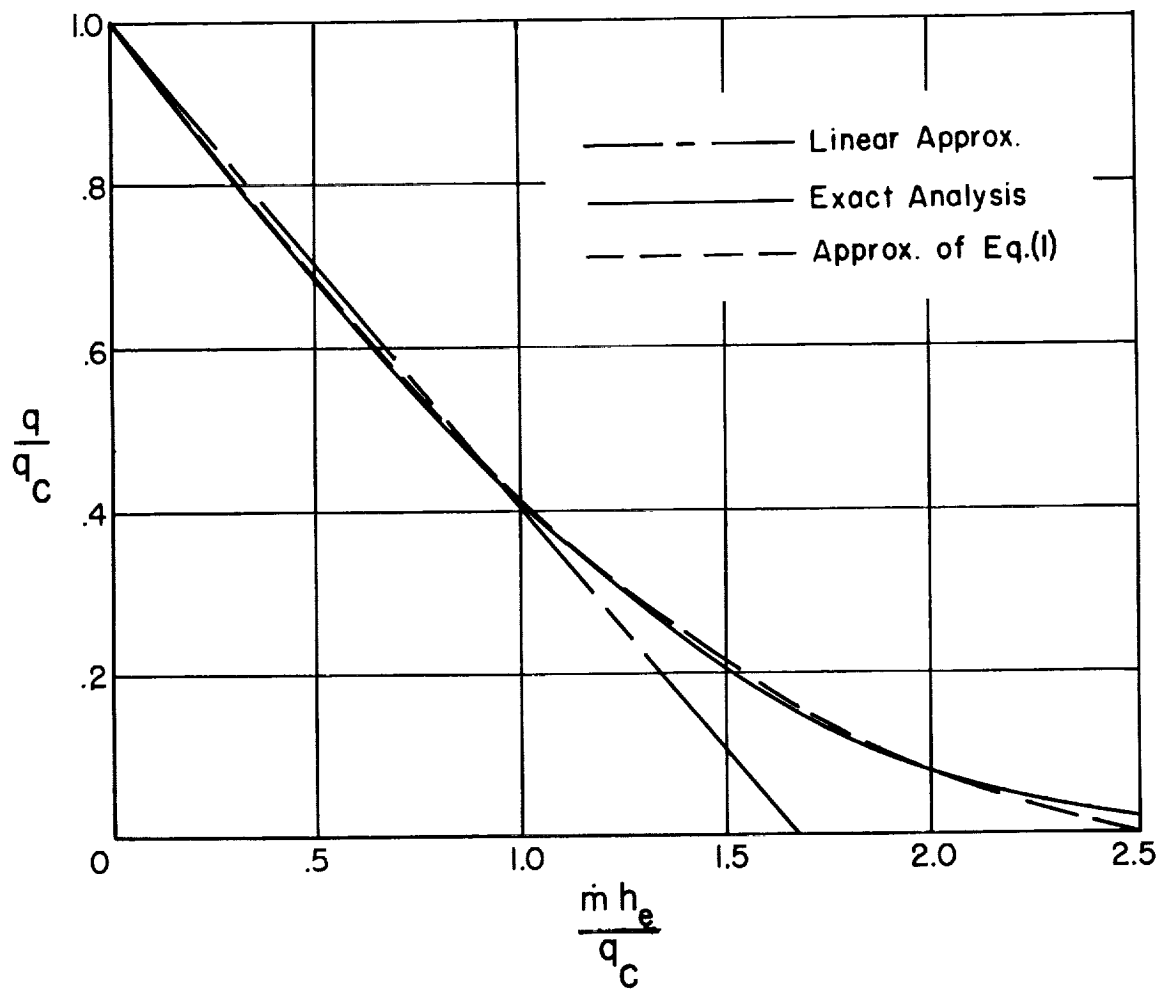


Figure 2.- Blocking effectiveness for a laminar boundary layer with air-to-air injection.

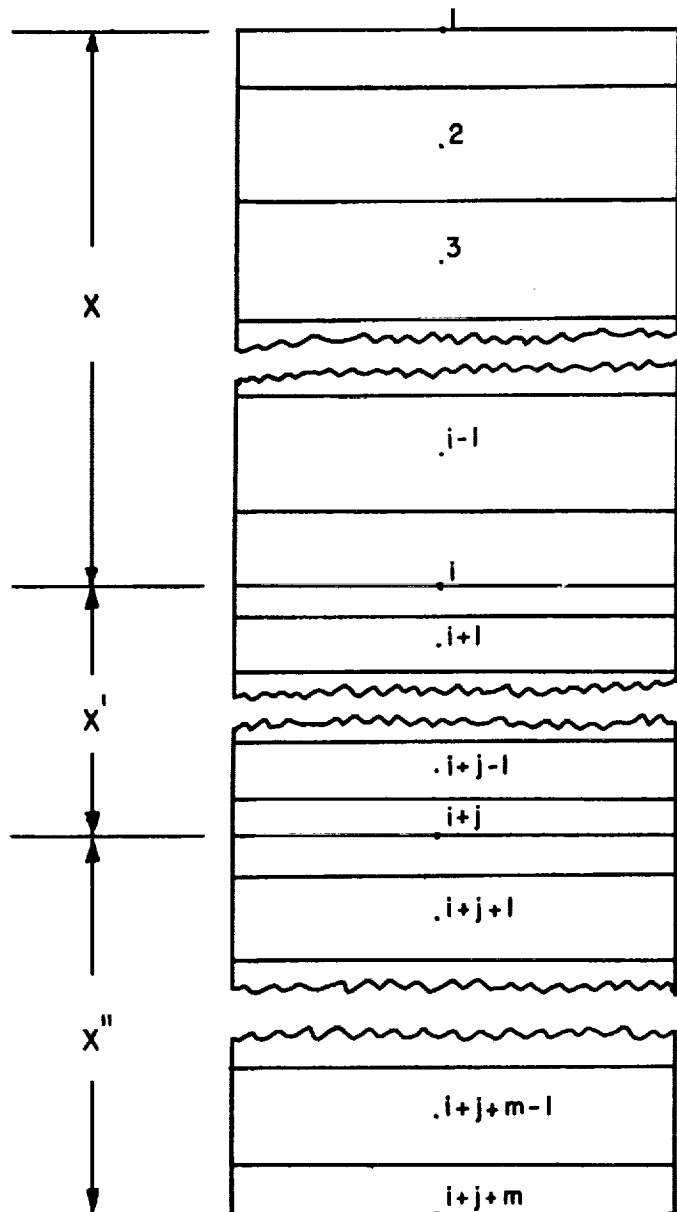
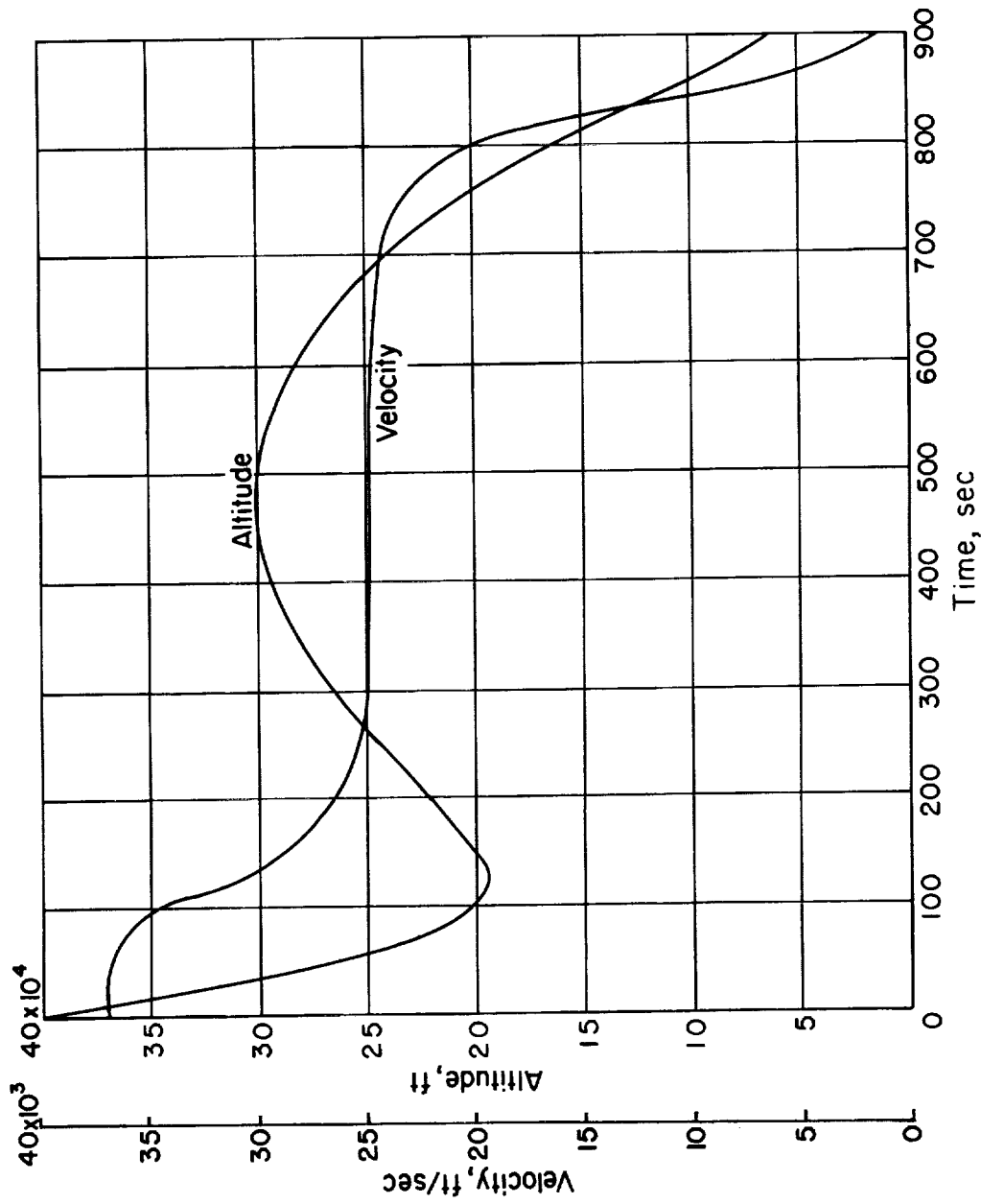
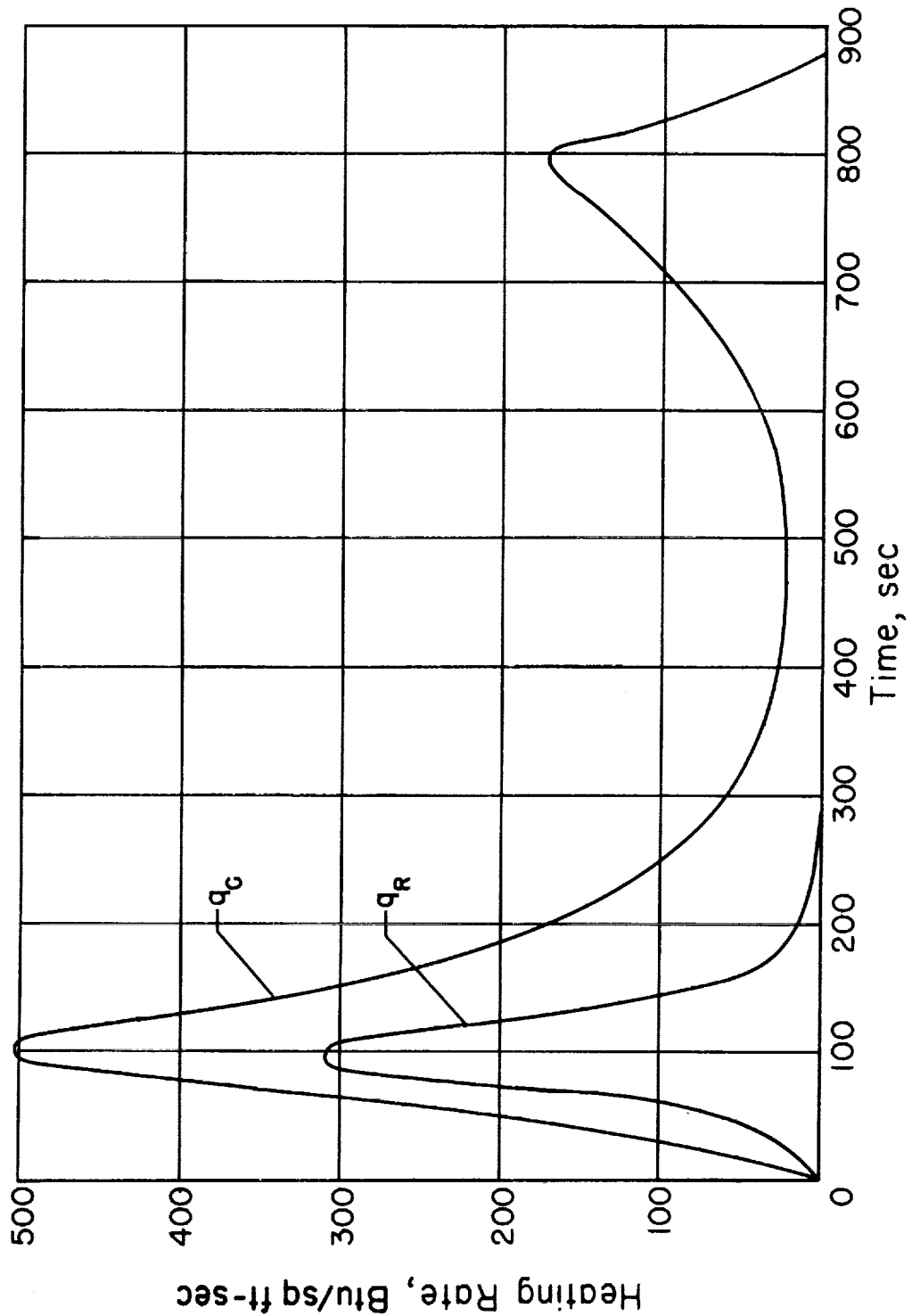


Figure 3.- Location of finite difference stations.



(a) Trajectory.

Figure 4.- Reentry at parabolic velocity.



(b) Heating rate.

Figure 4.- Concluded.

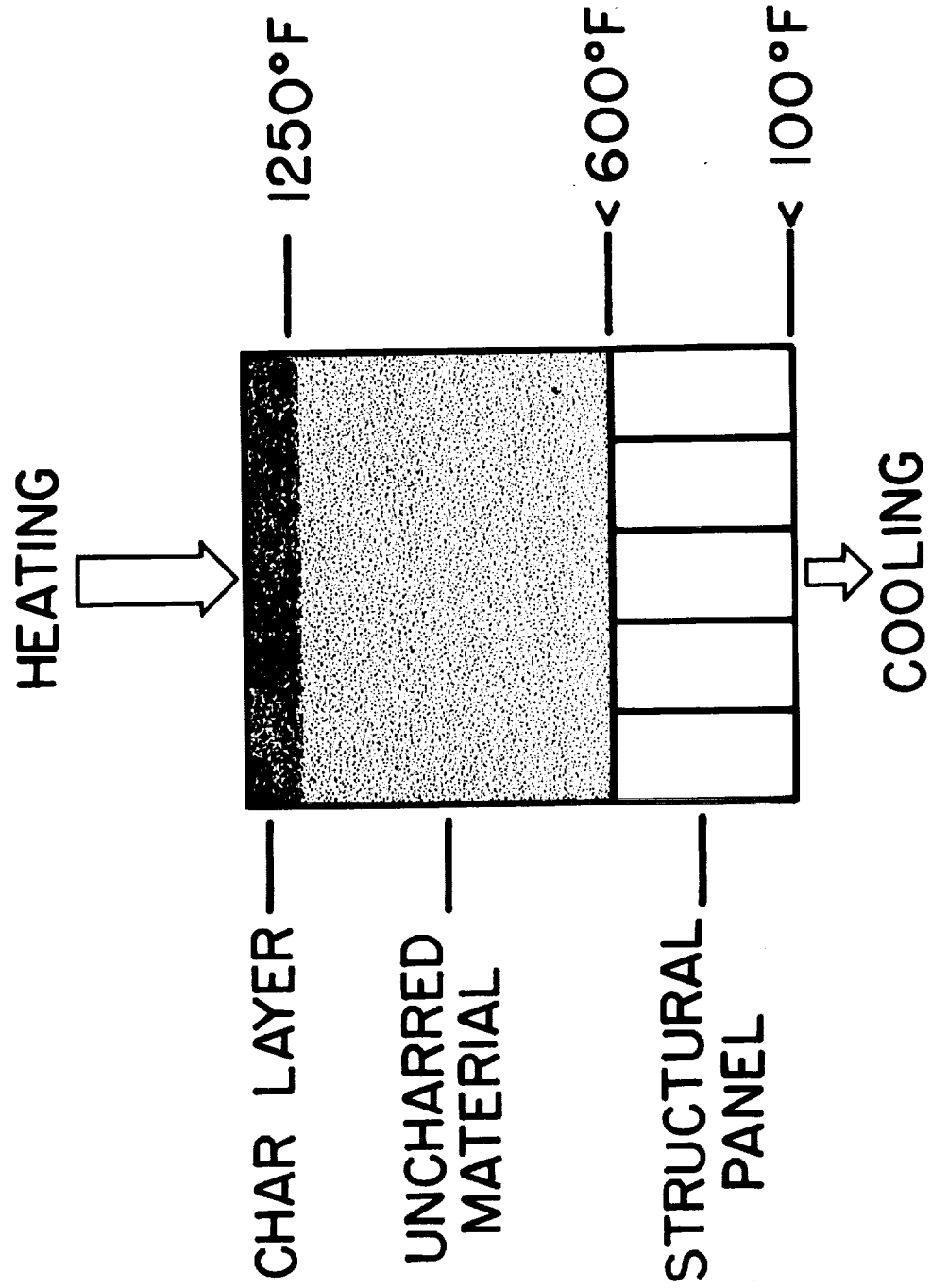
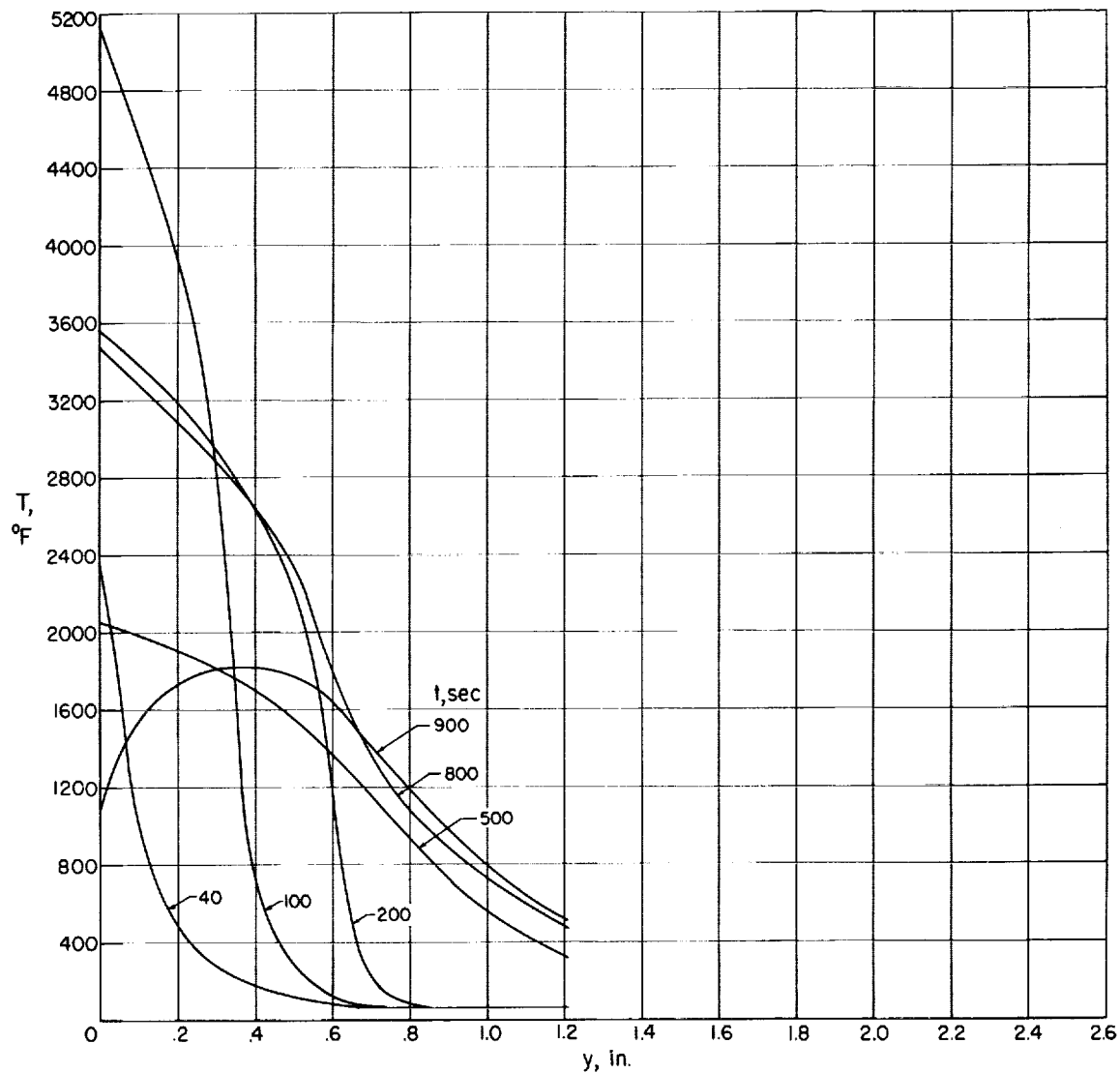


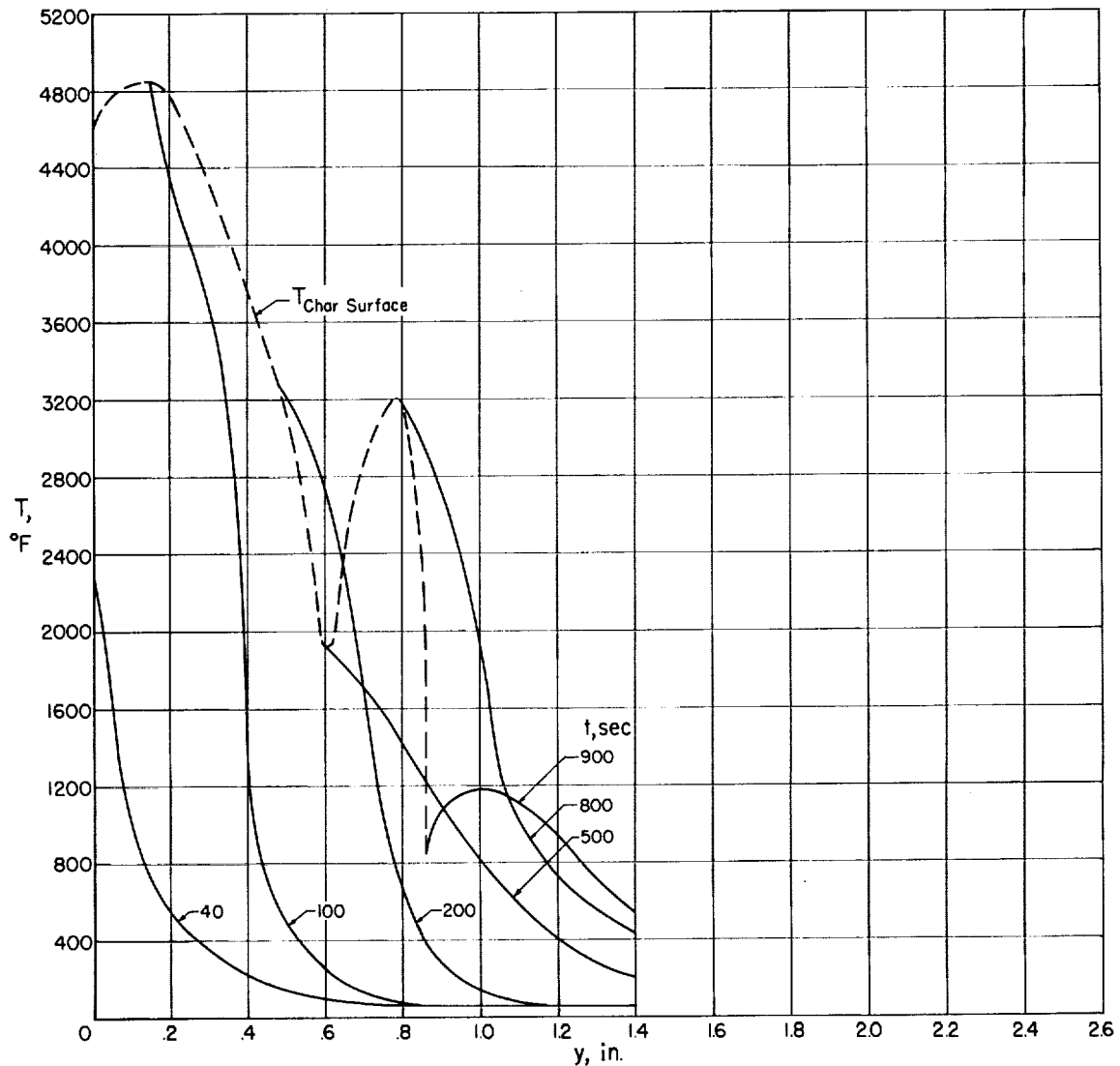
Figure 5.— Thermal protection system.



(a) No char loss; initial ablator thickness, 1.21 inches.

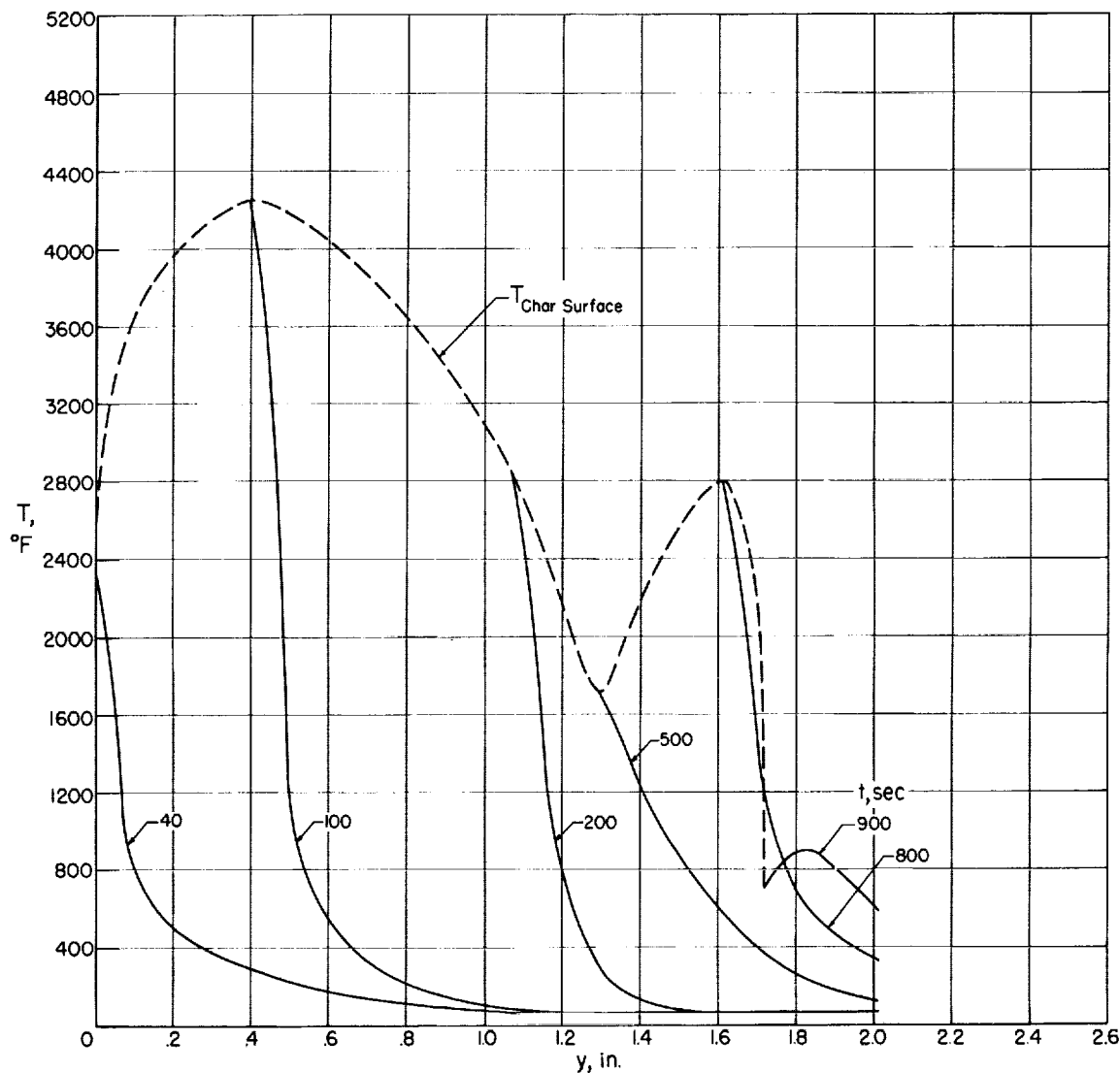
Figure 6.-- Temperature profiles.

L-1359



(b) 0.25-inch maximum char thickness; initial ablator thickness, 1.4 inches.

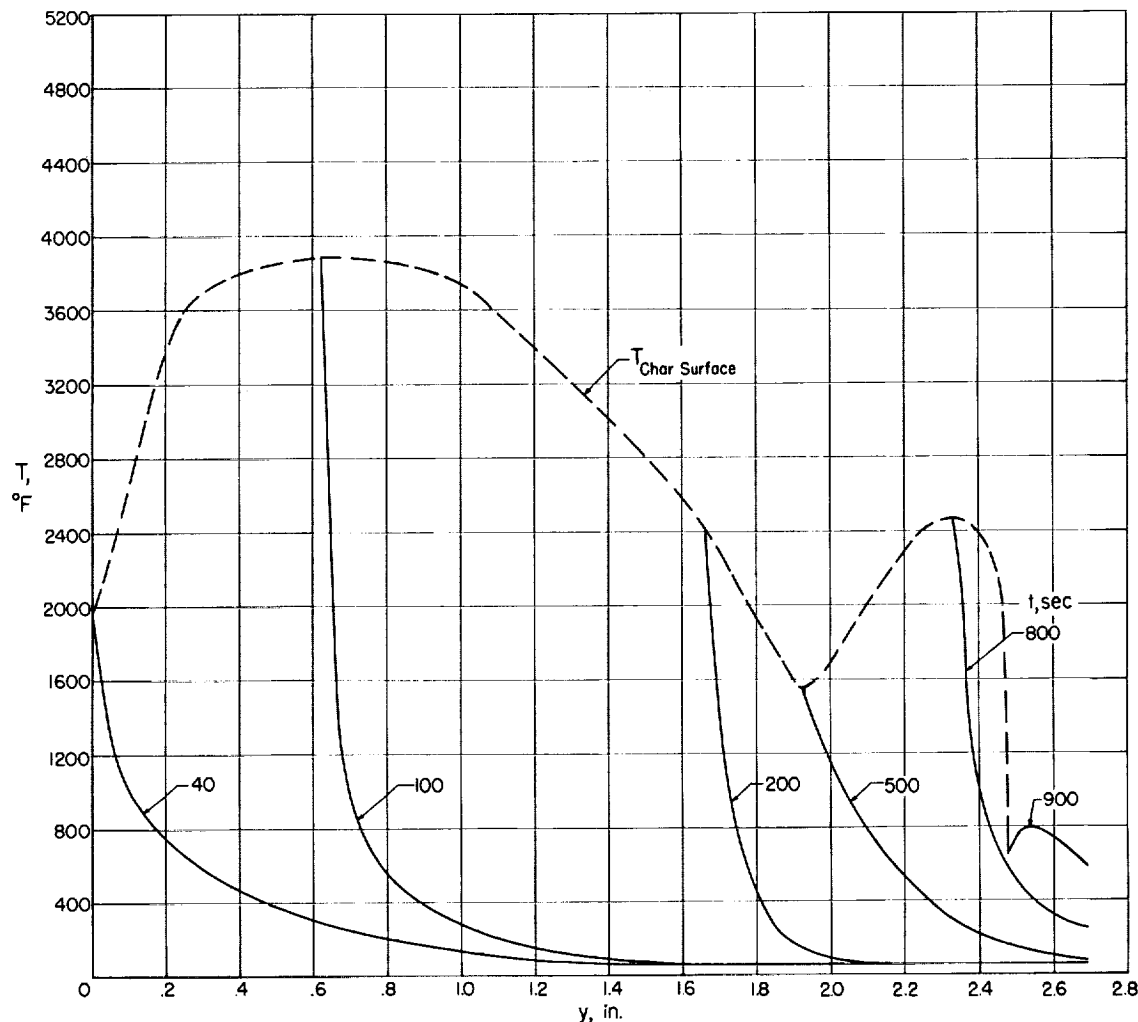
Figure 6.- Continued.



(c) 0.10-inch maximum char thickness; initial ablator thickness, 2.14 inches.

Figure 6.- Continued.

L-1359



(d) 0.05-inch maximum char thickness; initial ablator thickness, 2.69 inches.

Figure 6.- Concluded.

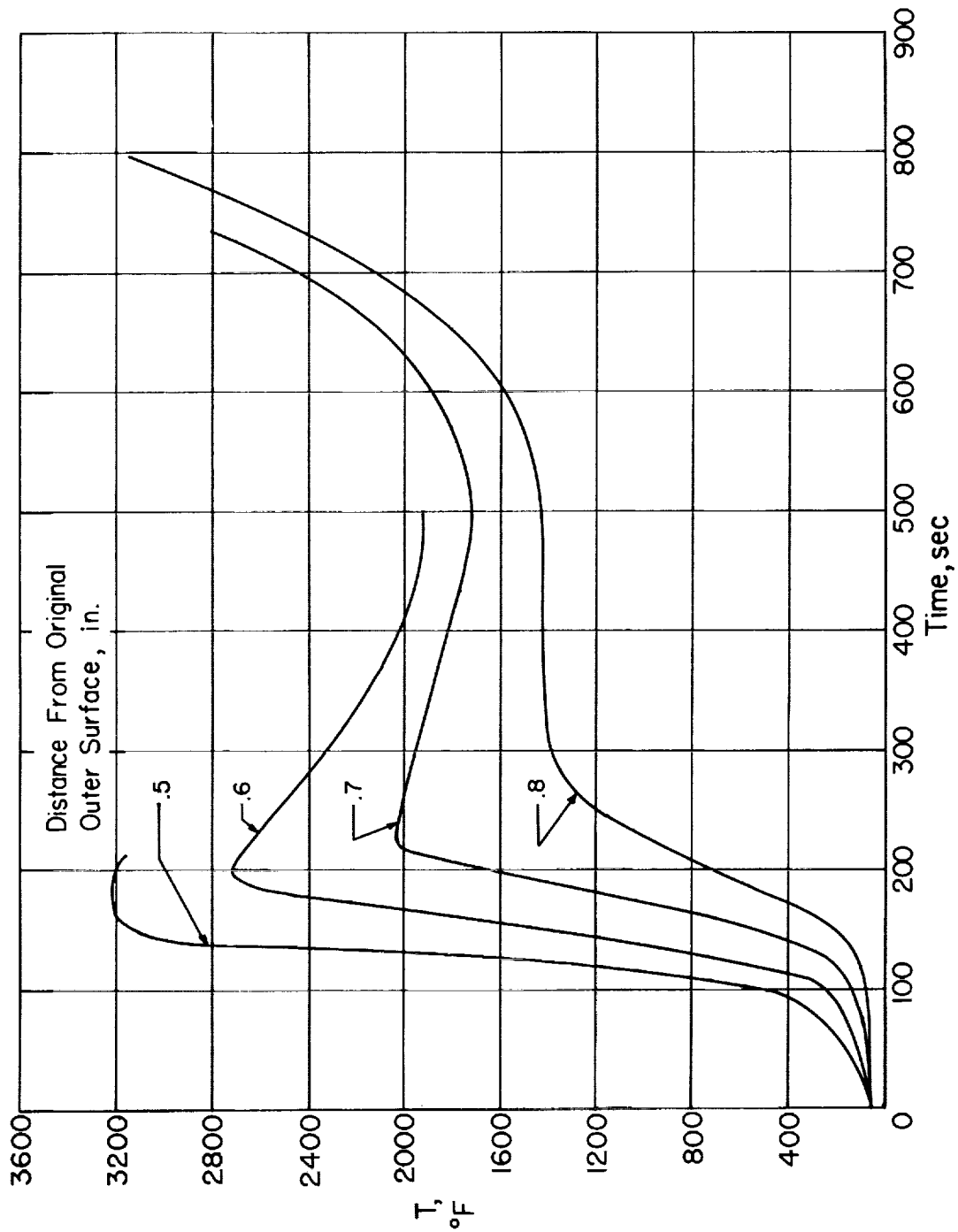


Figure 7.- Temperature histories. Maximum char thickness, 0.25 inch.

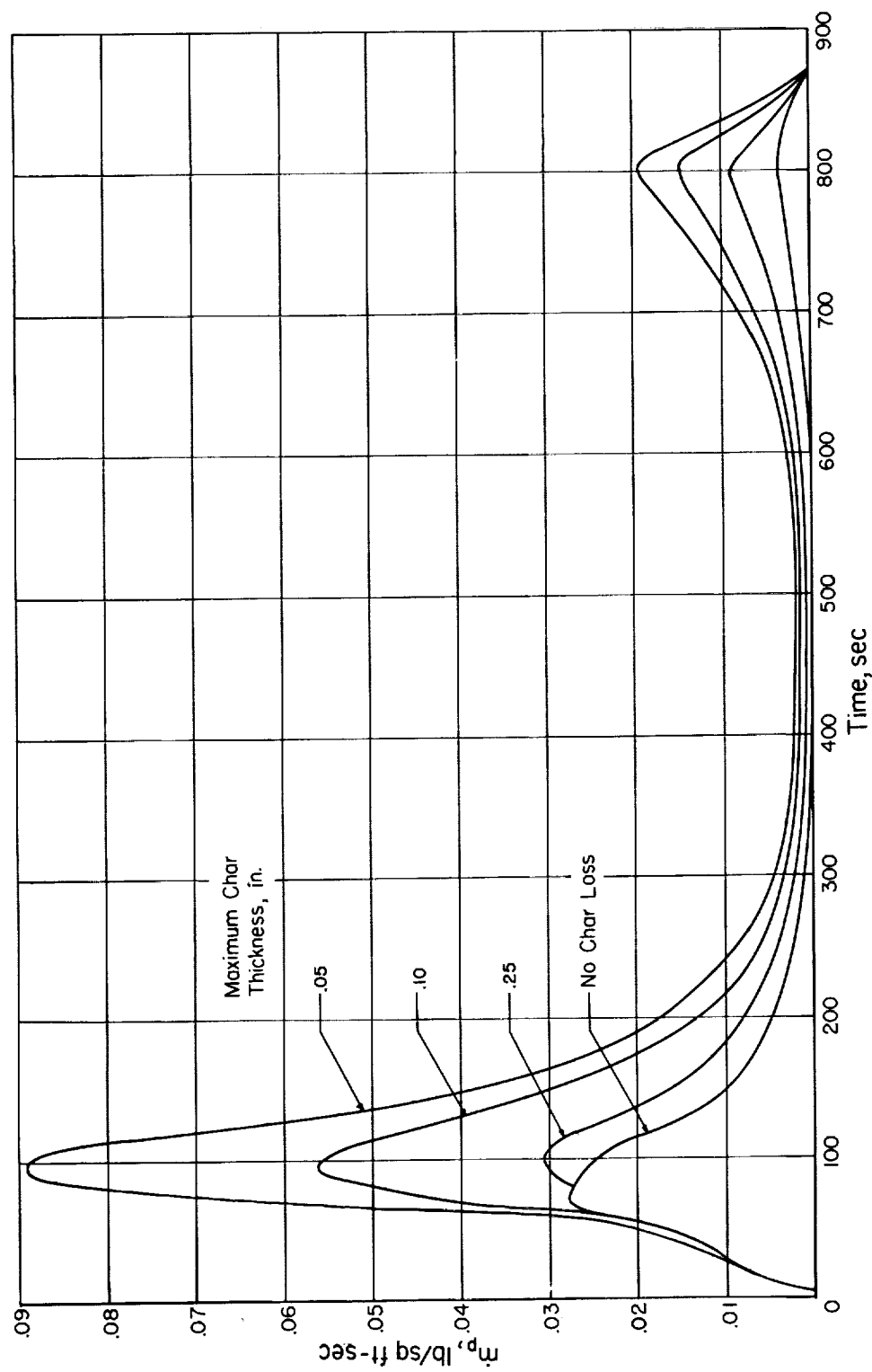


Figure 8.- Rate of pyrolysis.

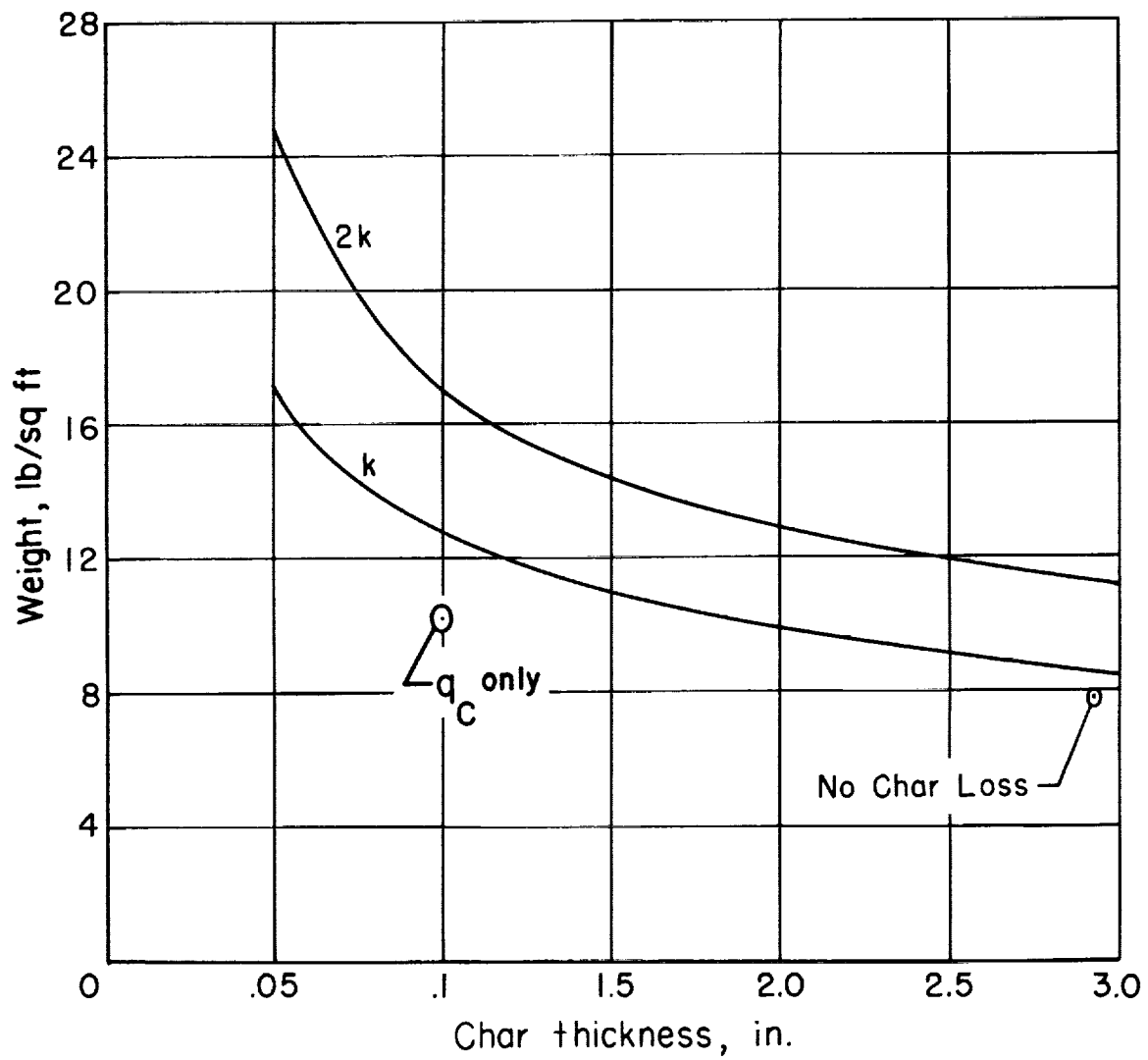


Figure 9.- Thermal-protection-system weight for 600° F bond temperature.
(k is thermal conductivity of char.)

L-1359

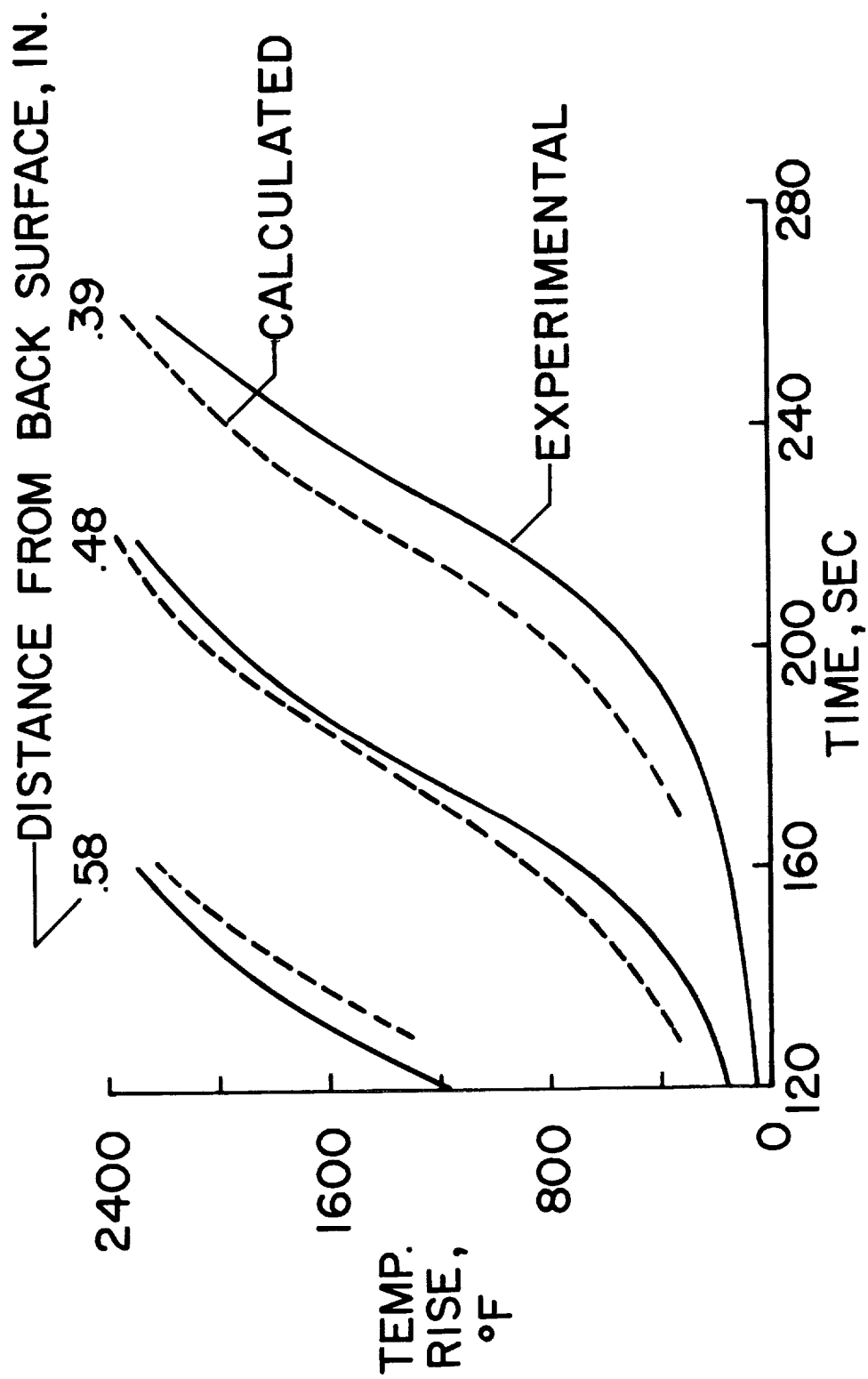


Figure 10. - Comparison of calculated and experimental temperature histories.



<p>NASA TN D-1370 National Aeronautics and Space Administration. NUMERICAL ANALYSIS OF THE TRANSIENT RESPONSE OF ADVANCED THERMAL PROTECTION SYSTEMS FOR ATMOSPHERIC ENTRY. Robert T. Swann and Claud M. Pittman. July 1962. 39p. OTS price, \$1.00. (NASA TECHNICAL NOTE D-1370)</p> <p>Equations for the transfer of heat through thermal protection shields are derived in finite difference form. These equations are applicable to charring ablatives, impregnated ceramics, subliming ablatives, heat sinks, and insulating materials and have been programmed for solution on a high-speed digital computer. In the program, thermal properties can be functions of temperature. Provision is made for analysis of heat shields subjected to simultaneous convective and radiative heat inputs. Some typical results are presented. Limited comparisons with experimental results are made.</p> <p>NASA</p>	<p>I. Swann, Robert T. II. Pittman, Claud M. III. NASA TN D-1370 (Initial NASA distribution: 2, Aerodynamics, missiles and space vehicles; 5, Atmospheric entry; 20, Fluid mechanics; 26, Materials, other.)</p> <p>Equations for the transfer of heat through thermal protection shields are derived in finite difference form. These equations are applicable to charring ablatives, impregnated ceramics, subliming ablatives, heat sinks, and insulating materials and have been programmed for solution on a high-speed digital computer. In the program, thermal properties can be functions of temperature. Provision is made for analysis of heat shields subjected to simultaneous convective and radiative heat inputs. Some typical results are presented. Limited comparisons with experimental results are made.</p> <p>NASA</p>
<p>NASA TN D-1370 National Aeronautics and Space Administration. NUMERICAL ANALYSIS OF THE TRANSIENT RESPONSE OF ADVANCED THERMAL PROTECTION SYSTEMS FOR ATMOSPHERIC ENTRY. Robert T. Swann and Claud M. Pittman. July 1962. 39p. OTS price, \$1.00. (NASA TECHNICAL NOTE D-1370)</p> <p>Equations for the transfer of heat through thermal protection shields are derived in finite difference form. These equations are applicable to charring ablatives, impregnated ceramics, subliming ablatives, heat sinks, and insulating materials and have been programmed for solution on a high-speed digital computer. In the program, thermal properties can be functions of temperature. Provision is made for analysis of heat shields subjected to simultaneous convective and radiative heat inputs. Some typical results are presented. Limited comparisons with experimental results are made.</p> <p>NASA</p>	<p>I. Swann, Robert T. II. Pittman, Claud M. III. NASA TN D-1370 (Initial NASA distribution: 2, Aerodynamics, missiles and space vehicles; 5, Atmospheric entry; 20, Fluid mechanics; 26, Materials, other.)</p> <p>Equations for the transfer of heat through thermal protection shields are derived in finite difference form. These equations are applicable to charring ablatives, impregnated ceramics, subliming ablatives, heat sinks, and insulating materials and have been programmed for solution on a high-speed digital computer. In the program, thermal properties can be functions of temperature. Provision is made for analysis of heat shields subjected to simultaneous convective and radiative heat inputs. Some typical results are presented. Limited comparisons with experimental results are made.</p> <p>NASA</p>

